JOURNAL OF SOLID STATE CHEMISTRY 51, 196–204 (1984)

Rate of Reactions between D_2O and $Ca_xAl_yO_z$

A. NØRLUND CHRISTENSEN*,† AND M. S. LEHMANN†

*Department of Inorganic Chemistry, Aarhus University, DK-8000 Aarhus C, Denmark, and †Institut Max von Laue–Paul Langevin, F-38042 Grenoble Cedex, France

Received April 5, 1983, and in revised form September 9, 1983

The rate of the reaction between D_2O and the calcium aluminum oxides $Ca_3Al_2O_6$, $Ca_5Al_6O_{14}$, $CaAl_2O_4$, and $CaAl_4O_7$ was investigated by on-line neutron diffraction powder methods at temperatures from room temperature to 100°C. The rate of the reaction increases with increasing calcium content of the compounds and with increasing temperature for each of the compounds. The crystallographic stable hydrate $Ca_3Al_2(OD)_{12}$ is obtained from $CaAl_4O_7$ and $CaAl_2O_4$ at temperatures above 63°C, from $Ca_5Al_6O_{14}$ at temperatures above 49°C, and from $Ca_3Al_2O_6$ at temperatures as low as 7°C.

Introduction

Powder neutron diffraction is well suited for the study of solid-state reactions in the crystalline state if the changes in structure or composition have a duration of at least a few hours. Because the absorption cross-section to most materials is low the neutrons can pass even bulky environment control units such as cryostats and furnaces, and the large size of the beam, and thus of the sample, ensures that the scattering gives a representative picture of the sample, even if this has inhomogeneities. In this respect neutrons are far superior to X rays for such analyses. In an on-line powder diffraction experiment the phase transitions or the chemical reactions in the specimen are measured in real time as these reactions and the diffraction process proceed simultaneously. An on-line neutron diffraction experiment requires a high flux reactor and a spectrometer with a multidetector. The use of X rays from a conventional X-ray tube would give a much too long exposure time for an on-line X-ray powder diffraction experiment that would only be adequate to perform with X rays from a syncrotron source. The crystallization of amorphous iron(III) hydroxide at hydrothermal conditions and the hydrogen–deuterium exchange between D_2O and solid γ-ALOOH were thus recently investigated using on-line neutron powder diffraction (*1, 2*). One type of reaction of extreme importance is the reaction of the metastable calcium silicates and calcium aluminates with water to produce stable hydrates. These processes, which occur when mixtures of cement and water solidify, typically have reaction times between a few hours and many years, and as they have not yet been studied by neutron powder diffraction we decided to undertake such a study.

In the pseudobinary system $CaO–Al_2O_3$ six crystalline compounds have been reported (*3, 4*) and are listed in Table I. In the literature concerning cement the formulae

0022-4596/84 $3.00

TABLE I

THE CRYSTALLINE COMPOUNDS FROM THE $CaO–Al_2O_3$ PSEUDOBINARY SYSTEM (*3, 4*)

Compound			Melting point (°C)	Crystallographic data	Ref.
$Ca_3Al_2O_6$	$3CaO \cdot Al_2O_3$	C_3A	1535[a]	Cubic $Pa3$	(*5*)
$Ca_{12}Al_{14}O_{33}$	$12CaO \cdot 7Al_2O_3$	$C_{12}A_7$	1455	Cubic $I\bar{4}3d$	(*4, 6*)
$Ca_5Al_6O_{14}$	$5CaO \cdot 3Al_2O_3$	C_5A_3	—	Orthorhombic $Cmc2_1$	(*7*)
$CaAl_2O_4$	$CaO \cdot Al_2O_3$	CA	1600	Monoclinic $P2_1/n$	(*8*)
$CaAl_4O_7$	$CaO \cdot 2Al_2O_3$	CA_2	1720	Monoclinic $C2/c$	(*9*)
$CaAl_{12}O_{19}$	$CaO \cdot 6Al_2O_3$	CA_6	1850[a]	Hexagonal	(*4, 10*)

[a] Melts incongruently.

of the compounds are often given as double oxides or as formulae with C for CaO, A for Al_2O_3, H for H_2O, and the formulae using these nomenclatures are also listed in Table I and will be used below. $C_{12}A_7$ is probably not an anhydrous compound in the strictest sense, and C_5A_3 is a metastable phase (*3*).

High alumina cement for the manufacturing of refractory concrete contains approximately 50–60% Al_2O_3, 30–40% CaO, and minor quantities of SiO_2 and Fe_2O_3 (*11*). High alumina cement can as well be made as white cements containing 72–80% Al_2O_3, 17–27% CaO, and almost without SiO_2 and Fe_2O_3 (*11*). A major constituent in high alumina cement is thus $CaAl_2O_4$ (CA). The calcium aluminum oxides react with water to form hydrates. At ordinary temperature the product of hydration of high alumina cement is $CaAl_2O_4 \cdot 10H_2O$ (CAH_{10}), and minor qualities of $Ca_2Al_2O_5 \cdot 8H_2O$ (C_2AH_8) (*12*). These two hydrates are hexagonal, but their crystal structures are not known. They are metastable and tend to change spontaneously to the stable hydrate $Ca_3Al_2O_6 \cdot 6H_2O$ (C_3AH_6) (*13*). This hydrate is cubic and its crystal structure is known (*14, 15*). The conversion of the metastable hexagonal hydrates to the stable cubic hydrate is accompanied by a change in volume, and these volume changes are the basis of the problems with the long-term strength of high alumina cement. At room temperature the change is slow and takes years. At high temperatures it may occur within a few weeks or even days. The conversion can be avoided by mixing the high alumina cement with $CaCO_3$. In that case the main hydration product is the compound $Ca_3Al_2O_6 \cdot CaCO_3 \cdot 11H_2O$, and this compound is stable in time and does not convert to C_3AH_6 (*13*). As for the oxides a shorthand notation exists for the hydrates listed in Table II. Even though the three main products of hydration are CAH_{10}, C_2AH_8, and C_3AH_6, other hydrates have been reported to occur. To get a more detailed picture of the hydration of some of the calcium aluminum oxides listed in Table I the hydration processes have been followed in real time using on-line neutron diffraction. The results of this investigation are reported below. The existence of the hydrate C_3AH_{12} has been questioned by Robson (*11*) and by Roberts (*23*), who suggest it to have the compositions $C_3A \cdot CaCO_3 \cdot 11H_2O$ and $C_3A \cdot CaCO_3 \cdot 12H_2O$, respectively.

Experimental

Sample preparation and characterization. The calcium aluminum oxides were made from pure CaO and Al_2O_3 (Merck 99.9%). The CaO was made from $Ca(OH)_2$ (Merck 99.9%) by heating in a crucible fur-

TABLE II

CRYSTALLINE COMPOUNDS FROM THE $CaO-Al_2O_3-H_2O$ PSEUDOTERNARY SYSTEM

Compound			Crystallographic data	Ref.
$Ca_4Al_6O_{13} \cdot 3H_2O$	$4CaO \cdot 3Al_2O_3 \cdot 3H_2O$	$C_4A_3H_3$	Orthorhombic *Abma*	(*16, 17*)
$Ca_3Al_2O_6 \cdot 6H_2O$	$3CaO \cdot Al_2O_3 \cdot 6H_2O$	C_3AH_6	Cubic *Ia3d*	(*14, 15*)
$Ca_2Al_2O_5 \cdot 6H_2O$	$2CaO \cdot Al_2O_3 \cdot 6H_2O$	C_2AH_6	Unknown	(*18*)
$Ca_2Al_2O_5 \cdot 8H_2O$	$2CaO \cdot Al_2O_3 \cdot 8H_2O$	C_2AH_8	Hexagonal	(*12, 19*)
$CaAl_2O_4 \cdot 10H_2O$	$CaO \cdot Al_2O_3 \cdot 10H_2O$	CAH_{10}	Hexagonal	(*12, 20, 21*)
$Ca_3Al_2O_6 \cdot 12H_2O$	$3CaO \cdot Al_2O_3 \cdot 12H_2O$	C_3AH_{12}	Unknown	(*11*)
$Ca_4Al_2O_7 \cdot 13H_2O$	$4CaO \cdot Al_2O_3 \cdot 13H_2O$	C_4AH_{13}	Trigonal *R3c* or $R\bar{3}c$	(*22*)
$Ca_4Al_2O_6CO_3 \cdot 11H_2O$	$3CaO \cdot Al_2O_3 \cdot CaCO_3 \cdot 11H_2O$	$C_3A\bar{C}H_{11}$	Hexagonal	(*13*)

nace at 1000°C for 8 hr. Stoichiometric mixtures of CaO and Al_2O_3 powders were mixed and pressed isostatically into rods at a pressure of 500 MPa (*24*). The rods to produce the compounds C_5A_3, CA, and CA_2 were zone melted and those to produce C_3A were zone sintered in a crystal growth furnace at a helium gas pressure of 0.1 MPa. Figure 1 shows a sketch of the experimental arrangement. The furnace is powered by a 200-kHz 30-kW RF generator and the heating coil heats a graphite ring that thermally heats the rod placed in the center of the graphite ring. The feed rod of the oxide mixture travels downward relative to the heating ring, and Fig. 1 illustrates a situation where most of the feed rod has been zone melted. The zone melted and zone sintered rods were crushed in a boron carbide mortar, and powders that could pass a 150-mesh sieve (~0.112 mm) were used in the investigation. Guinier powder patterns of the products were taken using Cu$K\alpha_1$ radiation and Si as an internal standard, and the photographs confirmed that the pure oxides C_3A, C_5A_3, CA, and CA_2 were obtained.

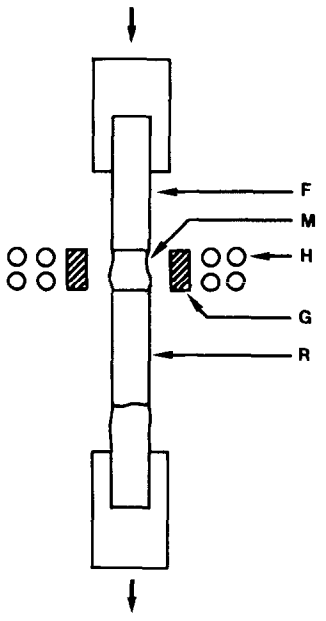

FIG. 1. Sketch of an experimental arrangement for zone melting of calcium aluminum oxide. The letters indicate the (F) oxide feed rod, (M) melt, (G) graphite ring, (H) heating coil, and (R) recrystallized oxide.

Neutron diffraction powder patterns. In a typical experiment 3.00 g of the pure oxide powder was mixed with 3.75 ml D_2O (99.7%) in an 11-mm-diameter vanadium container. The container was closed with an indium gasket to avoid loss of D_2O during the diffraction experiment. The neutron diffraction powder pattern was measured at the diffractometer D1B of the Laue–Langevin Institute with the container placed in a thermostatted vanadium oven with a temperature stability of 1.0°C (*1, 2*). The diffractometer has a 400-cell multidetector covering 80° in 2θ. The experiments were started immediately after the solid was mixed with D_2O by rapid heating of the

container in hot water, followed by transfer to the oven at the spectrometer table when the container had reached the same temperature as that of the oven. The neutron diffraction powder patterns were recorded repeatedly and were extracted at 6-, 12-, and 18-min intervals, depending upon the rates of the reactions. In Table III are listed the temperatures used in the on-line neutron diffraction experiments. The reactions proceed rather slowly at room temperature and the experiments performed at 30°C were thus made on specimens that were kept in a thermostate at 30°C. Powder patterns of these specimens were recorded at selected time intervals (of the order of 6–12 hr). The experiments listed for 7°C were only used to identify the end product for the reactions of C_3A and CA with D_2O at that temperature. The two specimens were kept in a refrigerator for 14 days prior to recording the powder pattern.

X-Ray Guinier powder patterns of the different hydrates formed in the diffraction experiments were recorded. The Guinier photographs, the neutron diffraction powder patterns, and the ASTM powder index files were used to identify the calcium aluminum oxide hydrates formed in the diffraction experiments. The results are listed in Table III.

The amount of remaining starting material and hydrate formed was determined for each diffraction pattern from the intensities of the diffraction lines of the two solid materials. The intensities were determined using the integration program by Wolfers (*25*). For each of the two components of a diffraction pattern, the sum of the intensities is proportional to the amount of component present, and the quantity of the specimen (solid and D_2O) is constant during a diffraction experiment. The variation in the sum of the intensities of a component therefore indicates the variation of its quantity with time. A total of 681 diffraction diagrams were used in the investigation. Figure 2 is an example of a diffraction pattern from the start of an experiment. It shows a broad scattering contribution from D_2O superimposed with the Bragg reflections of the starting material C_3A. Figure 3 is the last diffraction pattern of the experiment, showing a much smaller scattering contribution from D_2O than Fig. 2. This is to be expected as D_2O is consumed in the hydration process. Superimposed on the D_2O scattering contributions are the Bragg reflections from C_3AD_6.

TABLE III

EXPERIMENTAL TEMPERATURE AND REACTION PRODUCTS FOR EXPERIMENTS

Temp. (°C)	On-line diffraction	Compounds reached with D_2O			
		C_3A	C_5A_3	CA	CA_2
100	Yes			C_3AD_6	
90	Yes	C_3AD_6	C_3AD_6	C_3AD_6	C_3AD_6
75	Yes	C_3AD_6	C_3AD_6	C_3AD_6	C_3AD_6
63	Yes	C_3AD_6	C_3AD_6	C_3AD_6	C_3AD_6
49	Yes	C_3AD_6	C_3AD_6	C_3AD_{12}	C_3AD_{12}
30	No	C_3AD_6	C_2AD_6	C_3AD_{12}	C_3AD_{12}
26	Yes	C_3AD_6			
7	No	C_3AD_6		CAD_{10}	

Note. C = CaO, A = Al_2O_3, D = D_2O.

Results and Discussion

Table III shows the results of the hydration reactions between D_2O and the calcium

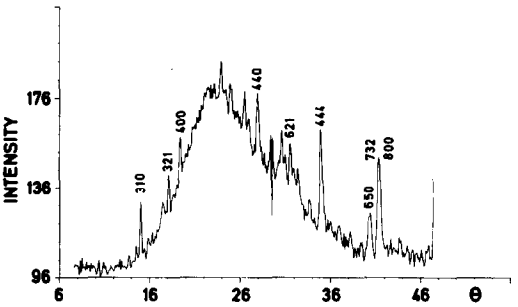

FIG. 2. Diffraction pattern at the start of the reaction between C_3A and D_2O at 30°C. The Miller indices for the strongest C_3A reflections are indicated.

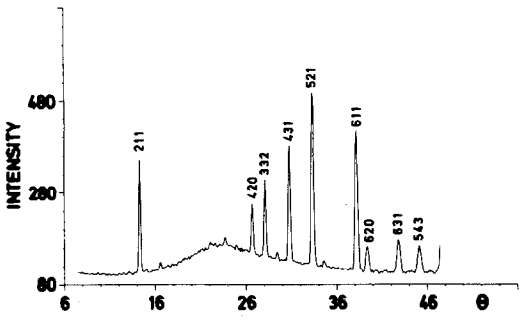

FIG. 3. Diffraction pattern showing Bragg reflections of the end product C_3AD_6 from the reaction between C_3A and D_2O at 30°C. The Miller indices for the strongest reflections are indicated.

aluminum oxides C_3A, C_5A_3, CA, and CA_2. For all the temperatures investigated C_3A yields the hexahydrate C_3AD_6. The same hydrate is also formed from D_2O and C_5A_3 at temperatures of 49°C and above, and from CA and CA_2 at temperatures of 63°C and above. It is thus possible to obtain the stable hexahydrate C_3AD_6 directly in hydration of the four compounds with D_2O by an adequate choice of the reaction temperature. At 30°C C_5A_3 reacted with D_2O to give the hydrate C_2AD_6. The existence of this hydrate was deduced from the X-ray powder pattern, which was in acceptable agreement with that reported on the ASTM index card 12-8 for the compound C_2AH_6. It is interesting that this hexahydrate C_2AD_6 is obtained in the experiment in preference to the octahydrate C_2AD_8 as the C_2A to D_2O ratio in the specimen was more than sufficient to yield the octahydrate, and as Carlson (*18*) obtained C_2AH_6 from C_2AH_8 by drying over calcium chloride. At 30 and 49°C, CA and CA_2 reacted with D_2O to form the dodecahydrate C_3AD_{12}. This hydrate was also identified from its X-ray powder pattern (ASTM index card No. 2-83). It is possible that this hydrate is identical with the H-phase reported by Ponomarev *et al.* (*16*). At 7°C CA and D_2O reacted with each other to form the decahydrate CAD_{10}. The compound was identified from its X-ray diffraction powder pattern (ASTM index card No. 12-408).

Figure 4 displays the intensity of C_3AD_6 vs time from the reaction of C_3A with D_2O at 90 and 63°C. C_3A reacts very fast with D_2O at these temperatures, and even the first diffraction pattern recorded in the experiment shows no Bragg reflections from C_3A. During a time period of ½ hr the intensities of C_3AD_6 increase to an apparently constant value. The fact that C_3A disappears in the reaction with D_2O before C_3AD_6 reaches its full scattering intensity indicates the formation of an intermediate amorphous phase in the reaction of C_3A with D_2O. The hexahydrate C_3AD_6 then crystallizes from this amorphous phase. Figure 5 displays the intensity of C_3AD_6 vs time from the reactions of C_3A with D_2O at 75, 49, and 25°C, and the intensity of C_3A at 49 and 25°C. Again, at 75°C the reaction between C_3A and D_2O is so fast that no Bragg reflections of C_3A can be observed in the first recorded diffraction diagram of this experiment. The intensity of C_3AD_6 increases during a time period of 1 hr to a high value. At 49 and 25°C, C_3A also reacts very fast with D_2O, but a small quantity of C_3A is observed in the first recorded diffraction patterns. C_3A is, however, consumed, and faster at 49 than at 25°C. The intensity of C_3AD_6 at 49 and 25°C increases rapidly at the start of the experiment, fol-

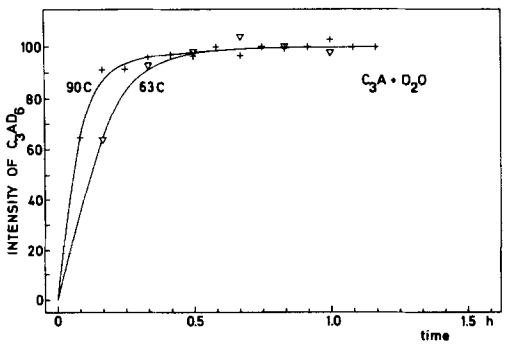

FIG. 4. Intensity of C_3AD_6 vs time from the reaction of C_3A with D_2O at 90°C (+), and 63°C (▽).

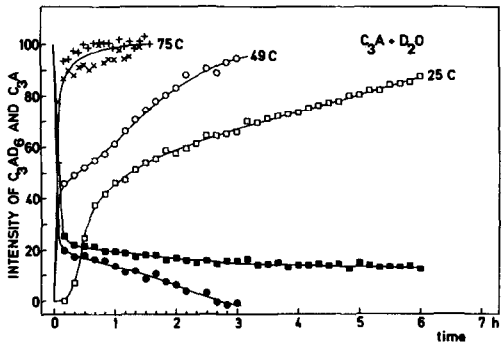

FIG. 5. Intensity of C_3AD_6 (×, +, ○, □) and C_3A (●, ■) vs time for the reaction of C_3A with D_2O at 75, 49, and 25°C. In this and the following figures filled symbols indicate the intensity of the start material and open symbols, the intensity of the products formed. Symbols of the same shape (□ and ■) in a figure correspond to product and start material in the same experiment. The time scale of Fig. 5 is approximately 4.5 times smaller than that of Fig. 4.

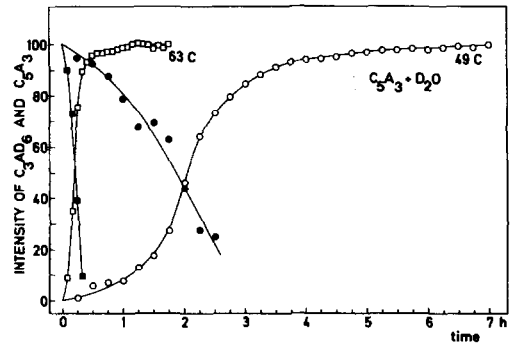

FIG. 7. Intensity of C_3AD_6 (□, ○) and C_5A_3 (■, ●) vs time for the reaction of C_5A_3 with D_2O at 63 and 49°C. The time scale of Fig. 7 is approximately three times smaller than that of Fig. 6.

lowed by a time period of steady growth, faster at 49 than at 25°C. This can be explained by the hypothesis that the first phase formed in the reaction of C_3A with D_2O is an amorphous phase from which crystals of C_3AD_6 grow.

Figures 6 and 7 display the intensity of C_3AD_6 and C_5A_3 for the reaction between D_2O and C_5A_3 at 90, 75, 63, and 49°C, respectively. The reaction is fast but the presence of C_5A_3 can be observed at the start of the experiments except for that performed at 90°C. The intensity of C_3AD_6 increases to an apparently constant level during the time period of the experiment at speeds that decrease with decreasing temperature. In this case also an amorphous phase may be formed as a precursor for the crystalline hexahydrate.

Figure 8 shows the intensities of C_3AD_6 for the reactions between CA and D_2O at 101, 89, 74, and 63°C. For the experiment performed at 101°C, CA was consumed so fast that it hardly could be observed in the first diffraction diagram. The reactions be-

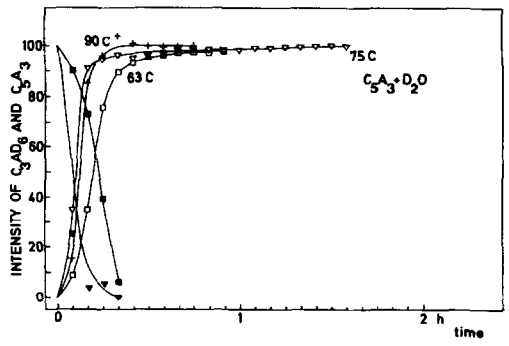

FIG. 6. Intensity of C_3AD_6 (+, ▽, □) and C_5A_3 (▼, ■) vs time for the reaction of C_5A_3 with D_2O at 90, 75, and 63°C.

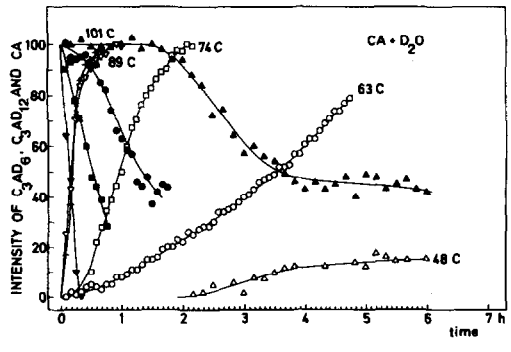

FIG. 8. Intensity of C_3AD_6 (+, ▽, □, ○) and CA (▼, ■, ●) vs time for the reaction of CA with D_2O at 101, 89, 74, and 63°C. For the experiment performed at 48°C the intensities of C_3AD_{12} (△) and of CA (▲) vs time are shown as well.

tween CA and D_2O are, however, slower than those between C_5A_3 and D_2O. The intensity of the hexahydrate C_3AD_6 increases smoothly during the time period of the experiment at a rate slower than that observed in the reactions between C_5A_3 and D_2O. Also displayed in the figure are the intensities of C_3AD_{12} and CA for the experiment performed at 48°C. The intensity of the dodecahydrate increases very slowly and the reflections of this phase are first observed in the diffraction patterns 2 hr after the start of the experiment. Figure 9 displays the intensities of C_3AD_6, C_3AD_{12}, and CA_2 for the reactions between CA_2 and D_2O performed at 93, 73, 63, and 49°C, respectively. The intensities of CA_2 decrease slowly, and those of C_3AD_6 and C_3AD_{12} increase slowly with time during the diffraction experiments. Again it may be assumed that an intermediate amorphous phase is formed as a precursor of the crystalline hydrates. The reaction between CA_2 and D_2O is much slower than the reaction between the other calcium aluminum oxides investigated and D_2O. This is obvious in Fig. 10 where the intensity of C_3AD_6 is displayed vs time for the reactions between the four calcium aluminum oxides and D_2O investigated at 63°C.

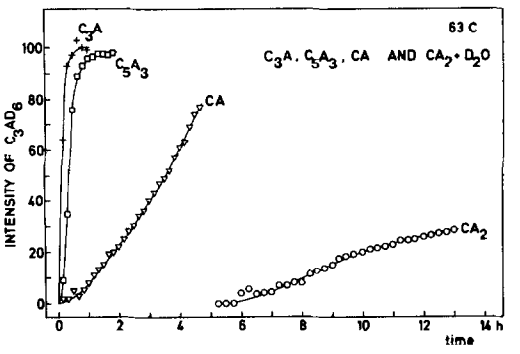

FIG. 10. Intensity of C_3AD_6 (+, □, ▽, ○) vs time for the reaction between D_2O and C_3A, C_5A_3, CA, and CA_2, respectively, performed at 63°C.

Figure 11 displays the intensities of the starting materials, except C_3A, and the hydrates formed in the experiment at 30°C. C_3A and C_5A_3 form the stable hexahydrate C_3AD_6 and its intensity increases during the entire time period of the experiment.

Conclusion

The processes of reactions of D_2O with C_3A, C_5A_3, CA, and CA_2 are possibly of the reconstructive type where bonds are broken and new bonds are formed. Unfortunately, only the crystal structure of the hydrate C_3AD_6 (hydrogrossular) is known in

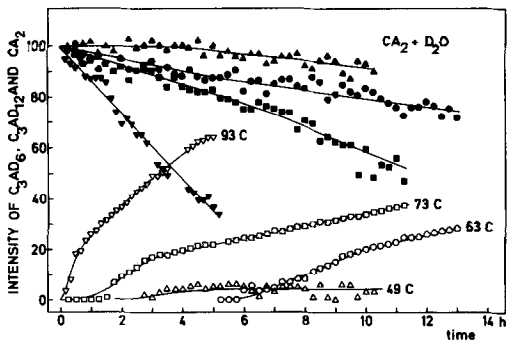

FIG. 9. Intensity of C_3AD_6 (▽, □, ○) and CA_2 (▼, ■, ●) vs time for the reaction of CA_2 with D_2O at 93, 73, and 63°C, respectively, and of C_3AD_{12} (△) and CA_2 (▲) vs time for the reaction performed at 49°C. The time scale of Fig. 9 is two times smaller than that of Fig. 8.

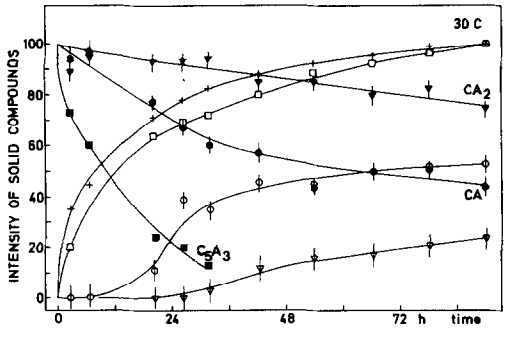

FIG. 11. Intensities of C_3AD_6 (+), C_2AD_6 (□), C_3AD_{12} (○ and ▽), C_5A_3 (■), CA (●), and CA_2 (▼) vs time for the reactions between C_3A, C_5A_3, CA, CA_2, and D_2O performed at 30°C. The intensity of C_3A disappeared almost immediately in the diffraction patterns at the start of the experiment.

great detail. In this structure aluminum is placed in $Al(OD)_6$ octahedra, and this cannot be the case in the pure calcium aluminum oxides. The process of hydration involves a rearrangement of atoms on the level of the coordination polyhedra, and the formula for C_3AD_6 is thus $Ca_3Al_2(OD)_{12}$. In the diffraction experiments involving the reactions between D_2O and C_3A it is obvious that C_3A disappears at a rate much greater than that at which C_3AD_6 is formed. This suggests the existence of an amorphous transition phase in the process of hydration of C_3A. This is probably also the case for the reactions of the three other solids with D_2O. For C_5A_3 it is best seen in Fig. 7 for the experiment at 49°C; for CA it is observed in Fig. 8 for the curves related to the 63°C data; and in the case of CA_2 Fig. 9 shows that the intensity of CA_2 decreases in the first 6 hr of the experiment performed at 63°C before the intensities of C_3AD_6 start to appear in the diffraction diagrams. The crystalline hydrates are then formed from the amorphous transition phase by processes involving nucleation and crystal growth the rate of which is possibly determined by diffusion; when the intensities of the hydrates formed at 30°C are displayed vs $\sqrt{t}$ (t is time in hours) (Fig. 12), roughly linear relations are observed at least for short times.

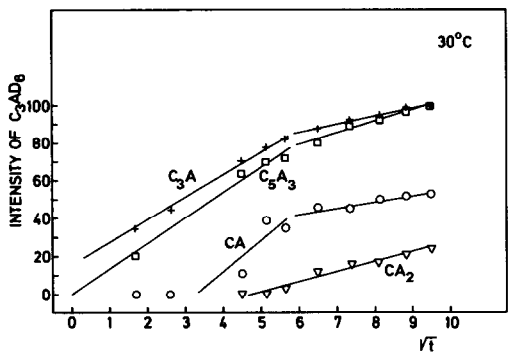

FIG. 12. Intensities of C_3AD_6, C_2AD_6, and C_3AD_{12} vs $\sqrt{t}$.

TABLE IV

TIME (hr) CONSUMED TO REDUCE THE QUANTITY OF THE CALCIUM ALUMINUM OXIDE TO HALF ITS ORIGINAL QUANTITY[a]

Temp. (°C)	C_3A	C_5A_3	CA	CA_2
100			<0.1	
90	<0.1	<0.1	0.2	3.5
75	<0.1	0.1	0.5	11.5
63	<0.1	0.3	1.3	25
49	<0.1	2	3.5	50[b]
30	<0.1	13	65	200[b]

[a] $t_{1/2}$ for the reactions of the calcium aluminum oxides with D_2O on a relative scale.
[b] Extrapolated.

In conclusion, it can be stated that the rates of hydration to crystalline products of the calcium aluminum oxides C_3A, C_5A_3, CA, and CA_2 with D_2O decrease in the sequence of the compounds given above. It is well known from the reactions of cement with water that the speed of reactions is strongly influenced by the composition of the cement. Grain size and grain size distribution of the solids will also be important factors for the rate of reactions of the solids with water. With this in mind, Table IV shows $t_{1/2}$, the time consumed to reduce the quantity of the calcium aluminum oxide to half its original quantity in the reaction with D_2O, derived from the intensities of the diffraction patterns of this investigation. It must be stressed that the numbers in Table IV only give $t_{1/2}$ on a relative scale for the four solids investigated.

Acknowledgments

The Danish Natural Science Research Council is acknowledged for financial support to one of us (A.N.C.). Mr. Niels Jørgen Hansen is acknowledged for preparation of the specimens, and Mr. A. Dorn, for assisting with the diffraction experiments.

References

1. A. N. CHRISTENSEN AND M. S. LEHMANN, *Acta Chem. Scand. A* **34**, 771 (1980).

2. A. N. CHRISTENSEN, M. S. LEHMANN, AND P. CONVERT, *Acta Chem. Scand. A* **36,** 303 (1982).
3. R. W. NURSE, J. H. WELCH, AND A. J. MAJUMDAR, *Trans. Brit. Ceram. Soc.* **64,** 409 (1965).
4. R. KIESSLING AND N. LANGE, *Jernkontorets Ann.* **149**(12), 855 (1963).
5. P. MONDAL AND J. W. JEFFREY, *Acta Crystallogr. B* **31,** 689 (1975).
6. National Bureau of Standards Circular 539, **9,** 20–22 (1959).
7. M. G. VINCENT AND J. W. JEFFREY, *Acta Crystallogr. B* **31,** 1422 (1978).
8. W. HÖRLENER AND HK. MÜLLER-BUSCHBAUM, *J. Inorg. Nucl. Chem.* **38,** 983 (1976).
9. D. W. GOODWIN AND A. J. LINDOP, *Acta Crystallogr. B* **26,** 1230 (1970).
10. DYSON, private commun., British Steel Corp., Swindow Labs., Rotterham (1972).
11. T. D. ROBSON, *In* "The Chemistry of Cement" (H. F. W. Taylor, Ed.), Vol. 2 p. 3, Academic Press, London/New York (1962).
12. F. G. Buttler and H. F. W. Taylor, *Cemento* **75,** 147 (1978).
13. M. Murat, A. Negro, and A. Bachiorrini, *C.R. Acad. Sci. Paris* **291,** 287 (1980).
14. C. COHEN-ADDAD, P. DUCROS, AND E. F. BERTAUT, *Acta Crystallogr.* **23,** 220 (1967).
15. H. BARTL, *Neues Jahrb. Mineral. Monatsh.* **H9,** 404 (1969).
16. V. I. PONOMAREV, B. N. LITVIN, AND N. V. BELOV, *Inorg. Mater.* **6,** 1459 (1971).
17. V. I. PONOMAREV, D. M. KHEIKER, AND N. V. BELOV, *Inorg. Mater.* **7,** 1591 (1972).
18. E. T. CARLSON, *J. Res. Nat. Bur. Stand.* **61,** 1 (1958).
19. A. NEGRO, L. CUSSINO, AND A. BACCHIORRINI, *Cemento* **75,** 285 (1978).
20. P. GALTIER, B. GUILHOT, M. MURAT, A. BACCHIORRINE, AND A. NEGRO, "7' Congr. Intern. Chim. des Céments, Septina, Paris, 1980," Vol. II, p. II/214.
21. H. F. W. TAYLOR, *In* "The Chemistry of Cement" (H. F. W. Taylor, Ed.), Vol. 2, p. 347, Academic Press, London/New York (1962).
22. S. J. AHMED AND H. F. W. TAYLOR, *Nature (London)* **215,** 622 (1967).
23. M. H. ROBERTS, *J. Appl. Chem.* **7,** 543 (1957).
24. A. N. Christensen, *J. Cryst. Growth* **33,** 99 (1976).
25. P. WOLFERS, "Programs for Treatment of Powder Profiles," private communication (1975).